

Inhibition of SARS-CoV-2 in Vero cell cultures by peptide-conjugated morpholino oligomers

Kyle Rosenke¹, Shanna Leventhal¹, Hong M. Moulton², Susan Hatlevig², David Hawman¹, Heinz Feldmann¹ and David A. Stein^{2*}

¹Laboratory of Virology, Division of Intramural Research, National Institute of Allergy and Infectious Diseases, National Institutes of Health, Hamilton, MT, USA; ²Department of Biomedical Sciences, Carlson College of Veterinary Medicine, Oregon State University, Corvallis, OR, USA

*Corresponding author. E-mail: dave.stein@oregonstate.edu

Received 28 July 2020; accepted 2 October 2020

Background: As the causative agent of COVID-19, SARS-CoV-2 is a pathogen of immense importance to global public health. Development of innovative direct-acting antiviral agents is sorely needed to address this virus. Peptide-conjugated morpholino oligomers (PPMO) are antisense compounds composed of a phosphorodiamidate morpholino oligomer covalently conjugated to a cell-penetrating peptide. PPMO require no delivery assistance to enter cells and are able to reduce expression of targeted RNA through sequence-specific steric blocking.

Methods: Five PPMO designed against sequences of genomic RNA in the SARS-CoV-2 5'-untranslated region and a negative control PPMO of random sequence were synthesized. Each PPMO was evaluated for its effect on the viability of uninfected cells and its inhibitory effect on the replication of SARS-CoV-2 in Vero-E6 cell cultures. Cell viability was evaluated with an ATP-based method using a 48 h PPMO treatment time. Viral growth was measured with quantitative RT-PCR and TCID₅₀ infectivity assays from experiments where cells received a 5 h PPMO treatment time.

Results: PPMO designed to base-pair with sequence in the 5' terminal region or the leader transcription regulatory sequence region of SARS-CoV-2 genomic RNA were highly efficacious, reducing viral titres by up to 4–6 log₁₀ in cell cultures at 48–72 h post-infection, in a non-toxic and dose-responsive manner.

Conclusions: The data indicate that PPMO have the ability to potently and specifically suppress SARS-CoV-2 growth and are promising candidates for further preclinical development.

Introduction

There is a pressing need for the development of additional direct-acting antiviral agents to address infections with SARS-CoV-2, the causative agent of COVID-19. Peptide-conjugated morpholino oligomers (PPMO) are single-stranded nucleic acid analogues capable of entering cells without assistance and interfering with gene expression through steric blockade of targeted RNA. PPMO are composed of a phosphorodiamidate morpholino oligomer (PMO) covalently conjugated to a cell-penetrating peptide (CPP).^{1–3} PPMO are water soluble, nuclease resistant and non-toxic at effective concentrations across a range of *in vitro* and *in vivo* applications.^{1,4} In several *in vivo* models of respiratory viruses, including influenza A virus,^{5,6} respiratory syncytial virus⁷ and porcine reproductive and respiratory syndrome virus,⁸ intranasally administered PPMO targeted against virus sequence have reduced viral titre and pathology in lung tissue.

The 5' untranslated region (5'UTR) of the coronavirus genome contains sequences and structures known to be important in various aspects of the virus life cycle, including translation and RNA synthesis.⁹ In previous studies, PPMO targeted to various sites in the 5'UTR of mouse hepatitis virus^{10,11} and SARS-CoV¹² were effectively antiviral. In the present study we investigated the ability of five PPMO targeted against various sites in the 5'UTR and polyprotein 1a/b translation start site (AUG) region of SARS-CoV-2 to suppress virus growth in cell cultures. We found that PPMO targeting the 5' terminal region and the leader transcription regulatory sequence (TRS) region of genomic RNA were potent inhibitors of SARS-CoV-2 replication.

Materials and methods

Biosafety

Work with infectious SARS-CoV-2 was approved by the Institutional Biosafety Committee (IBC) and performed in high biocontainment at Rocky

Mountain Laboratories (RML), NIAID, NIH. Sample removal from high bio-containment followed IBC-approved Standard Operating Protocols.

PPMO synthesis

PPMO were synthesized by covalently conjugating the CPP (RXR)₄ (where R is arginine and X is 6-aminohexanoic acid) to PMO (Gene Tools LLC, Philomath, OR, USA) at the 3' end through a non-cleavable linker, by methods described previously.³

Cells and viruses

Vero-E6 cells (ATCC) were maintained in DMEM supplemented with 10% FCS, 1 mM L-glutamine, 50 U/mL penicillin and 50 µg/mL streptomycin (growth medium). All cell culture incubations were carried out at 37°C and 5% CO₂. SARS-CoV-2 isolate nCoV-WA1-2020 was kindly provided by the CDC (Atlanta, GA, USA). Preparation and quantification of the virus followed methods described previously.¹³ Briefly, the original virus stock was propagated once at RML in Vero-E6 cells in DMEM supplemented with 2% FBS containing L-glutamine and antibiotics as above (infection medium). The virus stock used in the experiments was passage 4 and was confirmed by next-generation sequencing to be identical to the initial deposited GenBank sequence MN985325.

Cell viability assay

Cell viability was assessed using CellTiterGlo (Promega). Vero-E6 cells grown to approximately 80% confluence in 96-well plates were incubated in the presence of PPMO in infection medium for 48 h, then assayed according to the manufacturer's instructions. Statistical analysis was carried out using GraphPad Prism (San Diego, CA, USA).

Antiviral assays

PPMO were resuspended in sterile PBS. Vero-E6 cells were plated in 48-well plates and were approximately 80% confluent on the day of infection. At 5 h before infection, the growth medium was removed and replaced with infection medium containing PPMO. For viral infections, the PPMO-containing medium was aspirated and the cells rinsed twice with DMEM before adding 100 µL of infection medium containing virus at an moi of 0.01. Following a 1 h infection period, the virus-containing inoculum was aspirated and the cells washed twice with infection medium, after which 300 µL of fresh infection medium without PPMO was added. At 12, 24, 48 and 72 h post-infection, all of the medium in each well was collected for quantitative RT-PCR (qRT-PCR) and TCID₅₀ analysis.

Evaluation of virus quantity by qRT-PCR

Supernatants were harvested as described above and viral RNA purified and quantified by using one-step qRT-PCR following methods described previously.¹³ Briefly, total RNA was isolated with the RNeasy Mini Kit (Qiagen) and RT-PCR carried out using the One-Step RT-PCR Kit (Qiagen) according to the manufacturer's protocols. Ct values were calculated using standards produced as described previously.¹³

TCID₅₀ evaluations

Viral supernatants were serially diluted in DMEM and each dilution sample was titrated in triplicate. Subsequently, 100 µL of each virus dilution was transferred to Vero-E6 cells grown in 96-well plates containing 100 µL of DMEM. Following a 7 day incubation period, wells were scored for cytopathic effect. The TCID₅₀ values were calculated via the Reed-Muench formula.

Results

PPMO design

PPMO design was guided by previous studies in which various nidoviruses were targeted with PPMO.^{10-12,14,15} In this study, five PPMO were designed to target the 5'UTR and first translation start site region of SARS-CoV-2 positive-sense genomic RNA (Table 1). Two of the PPMO target the 5' terminal region of the genome. Both 5'END-1 and 5'END-2 were designed with the intention of interfering with pre-initiation of translation of genomic and subgenomic mRNAs.

Coronaviruses produce a set of nested mRNAs through the process of discontinuous subgenomic mRNA synthesis. The TRS is a 6–10 nt sequence that is critical in the production of negative-strand mRNA templates during this process.^{16,17} For SARS-CoV (GenBank NC_004718), the leader-TRS core sequence consists of nt 67–72 of the genomic RNA¹⁸ and most if not all viral subgenomic mRNAs possess the same 72 nt 5' leader sequence. Two PPMO were designed to target the genomic 5'UTR region containing the putative SARS-CoV-2 leader-TRS core sequence (nt 70–75, 5'-ACGAAC-3') and thereby potentially interfere with body-TRS to leader-TRS base-pairing and/or with translocation of the 48S translation preinitiation complex along the 5'UTR of the genomic and subgenomic mRNAs.

The AUG PPMO was designed to target the translation initiation region for ORF1a/b, which codes for the replicase polyprotein, with the intention to block translation initiation.

Table 1. Names, sequences and target locations of SARS-CoV-2 PPMO

PPMO name	PPMO sequence (5'-3')	PPMO target location in the SARS-CoV-2 genome ^a
NC	CCTCTTACCTCAGTTACAATTTATA	not applicable (negative control)
5'END-1	CCTGGGAAGGTATAAACCTTTAAT	1–24
5'END-2	TGTTACCTGGGAAGGTATAAACCTT	5–29
TRS-1	TTTTAAAGTTTCGTTTAGAGAACAG	59–82
TRS-2	AAGTTCGTTTAGAGAACAGATCTAC	53–77
AUG ^b	AGGCTCTC CAT CTTACCTTTCGGT	251–275

^aBased on GenBank NC_045512.

^bBases targeting the AUG translation start site of SARS-CoV-2 1a/b polyprotein are in bold.

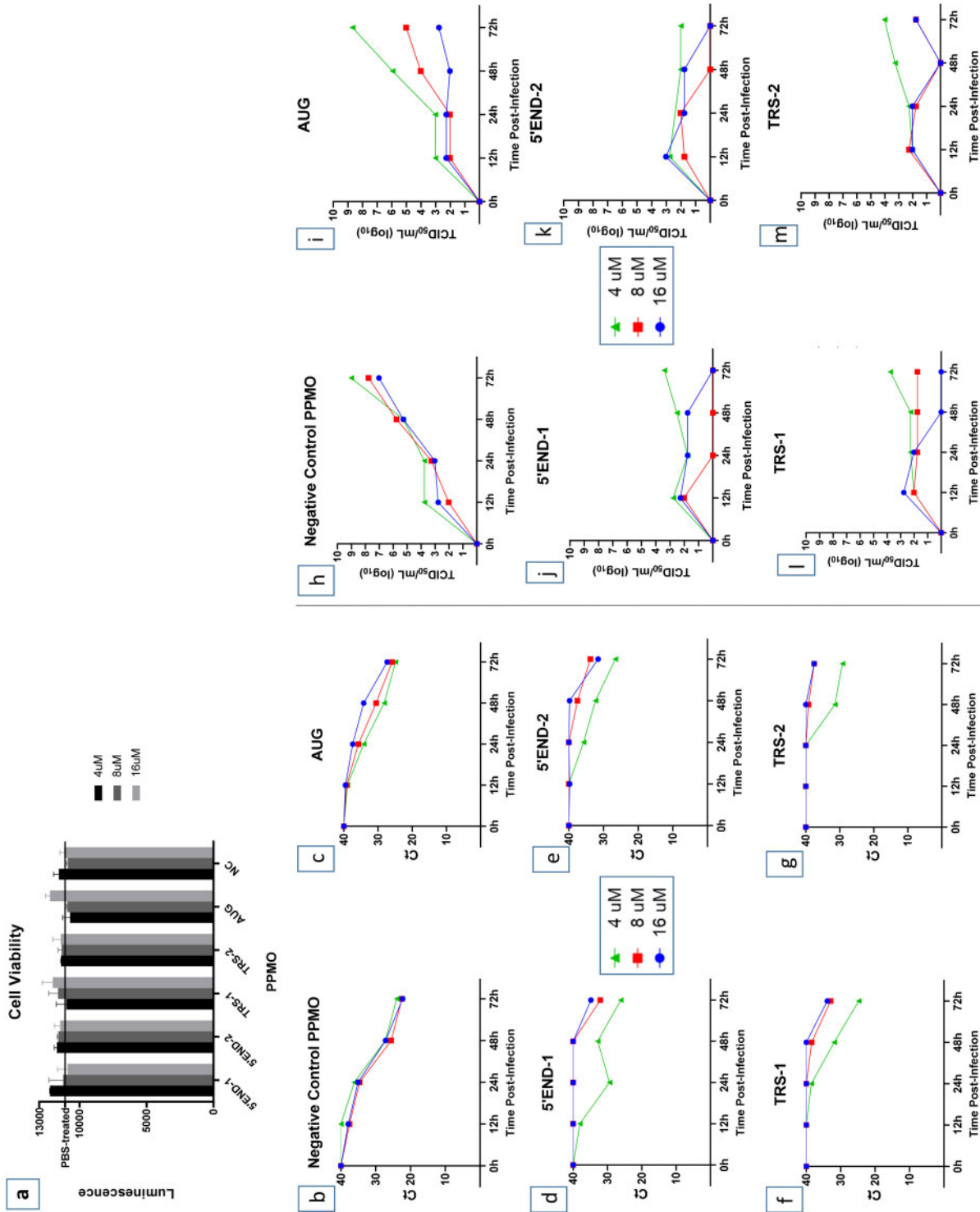


Figure 1. Effect of PPMO on cell viability and SARS-CoV-2 growth. (a) Evaluation of the effect of PPMO treatment on cellular ATP level, as an indicator of cell viability, was carried out using uninfected cells incubated for 48 h with increasing concentrations of the indicated PPMO. ATP levels were determined via luminescence readings and are shown compared with PBS-treated cells. For each PPMO concentration, triplicate samples were assayed and the mean±SD is shown. (b–m) Growth curves of SARS-CoV-2. Vero-E6 cells were treated with the indicated concentration of PPMO for 5 h before infection with SARS-CoV-2 (moi of 0.01), then incubated without PPMO after infection. Cell supernatants were collected at 12, 24, 48 and 72 h post-infection and analysed by qRT-PCR (b–g) or TCID₅₀/mL endpoint dilution (h–m) using three technical repeats. Cells treated with PBS had titres similar to those shown for NC PPMO. The limit of virus detection for the TCID₅₀ assay was 10¹/mL. This experiment was carried out twice, under similar conditions, yielding similar results, and the results from a single experiment are shown. This figure appears in colour in the online version of JAC and in black and white in the print version of JAC.

A negative control PPMO (NC), consisting of a random-sequence PMO conjugated to the same CPP used in the other PPMO, was included (see Table 1), to control for non-specific effects of the PPMO chemistry. NC was screened using BLAST and contains little significant homology to any primate, rodent or viral sequences.

Evaluation of PPMO cytotoxicity

To evaluate the effect of PPMO on cell viability, cells were treated under conditions similar to those used in the antiviral assays described below, but for a longer treatment time and in the absence of virus. Cells were treated in triplicate with increasing doses of PPMO for 48 h then evaluated with a quantitative cell viability assay. At the concentrations used in the antiviral assays described below, none of the PPMO produced more than a 5% cytotoxic effect (Figure 1a).

Evaluation of PPMO antiviral activity

To determine the inhibitory effect of the various PPMO on SARS-CoV-2 replication, Vero-E6 cells were treated with each of the six PPMO described in Table 1 at 4, 8 and 16 μM for 5 h before infection, then incubated without PPMO after infection. Cell supernatants were collected at four timepoints post-infection: 12, 24, 48 and 72 h. Virus growth was evaluated by two methods, qRT-PCR and TCID₅₀ infectivity assay. Using an moi of 0.01, virus growth rose steadily and reached peak growth at 72 h post-infection (Figure 1b and h). Growth of the virus under PBS treatment was highly similar to virus growth under NC PPMO treatment (data not shown). Four of the five PPMO designed to target SARS-CoV-2 RNA were highly effective, suppressing viral titres by 4–6 log₁₀ at the 48 and 72 h timepoints (Figure 1h–m). qRT-PCR analysis showed that in cells treated with 8 or 16 μM of any of the four PPMO targeting the 5' terminal or TRS regions, virus growth was markedly suppressed at 12–48 h post-infection (Figure 1b–g). The number of cycles required to detect virus from those samples was approximately the same as the number of cycles required to detect the input virus shortly after infection. At 72 h post-infection, the efficacy of the 5'END and TRS PPMO waned, to a minor extent, although still providing considerable suppression of virus growth. Overall, the AUG PPMO was less effective than the other four antiviral PPMO used in this study (Figure 1c and i).

Discussion

In this study, we found that PPMO targeting the 5' terminal region or leader-TRS region were highly effective at inhibiting the growth of SARS-CoV-2, whereas a PPMO targeting the polyprotein 1a/b AUG translation start site region was less effective. It is unknown if the AUG PPMO was less able to anneal to its target or if duplexing did occur yet was less consequential to virus growth.

To date, little sequence variation in the PPMO target sites in the 5'UTR of SARS-CoV-2 has been identified. Of the whole-genome nucleotide sequences reported in GenBank (at the time of writing), two genotypes contain a single mismatch with the 5'END PPMO and one genome has a single mismatch with the TRS PPMO.¹⁹ Previous studies have reported that PPMO having a single base

mismatch with their target site retain approximately 90% of their activity compared with those having perfect agreement.^{15,20}

This study demonstrates that PPMO targeted against SARS-CoV-2 can enter cells readily and inhibit viral replication in a sequence-specific, dose-responsive and non-toxic manner. As well, the PPMO exhibited durable potency, considering that only a 5 h PPMO treatment time was used. Our results here, in addition to the *in vivo* antiviral efficacy demonstrated by PPMO against several respiratory viruses in previous studies,^{5–8} suggest that further development of the 5'END and TRS PPMO to address SARS-CoV-2 infections is warranted.

Funding

This work was funded by the Intramural Research Program of the National Institute of Allergy and Infectious Diseases (NIAID), National Institutes of Health (NIH).

Transparency declarations

None to declare.

References

- Moulton HM, Moulton JD. Morpholinos and their peptide conjugates: therapeutic promise and challenge for Duchenne muscular dystrophy. *Biochim Biophys Acta* 2010; **1798**: 2296–303.
- Moulton HM, Moulton JD. Antisense morpholino oligomers and their peptide conjugates. In: Kurreck J, ed. *Therapeutic Oligonucleotides*. Royal Society of Chemistry, 2008; 43–79.
- Abes S, Moulton HM, Clair P et al. Vectorization of morpholino oligomers by the (R-Ahx-R)₄ peptide allows efficient splicing correction in the absence of endosomolytic agents. *J Control Release* 2006; **116**: 304–13.
- Stein DA. Inhibition of RNA virus infections with peptide-conjugated morpholino oligomers. *Curr Pharm Des* 2008; **14**: 2619–34.
- Gabriel G, Nordmann A, Stein DA et al. Morpholino oligomers targeting the PB1 and NP genes enhance the survival of mice infected with highly pathogenic influenza A H7N7 virus. *J Gen Virol* 2008; **89**: 939–48.
- Lupfer C, Stein DA, Mourich DV et al. Inhibition of influenza A H3N8 virus infections in mice by morpholino oligomers. *Arch Virol* 2008; **153**: 929–37.
- Lai SH, Stein DA, Guerrero-Plata A et al. Inhibition of respiratory syncytial virus infections with morpholino oligomers in cell cultures and in mice. *Mol Ther* 2008; **16**: 1120–8.
- Opriessnig T, Patel D, Wang R et al. Inhibition of porcine reproductive and respiratory syndrome virus infection in piglets by a peptide-conjugated morpholino oligomer. *Antiviral Res* 2011; **91**: 36–42.
- Masters PS, Perlman S. Coronaviridae. In: Knipe DM, Howley PM, eds. *Fields Virology*. Lippincott Williams & Wilkins, 2013; 825–58.
- Burrer R, Neuman BW, Ting JP et al. Antiviral effects of antisense morpholino oligomers in murine coronavirus infection models. *J Virol* 2007; **81**: 5637–48.
- Neuman BW, Stein DA, Kroeker AD et al. Antisense morpholino-oligomers directed against the 5' end of the genome inhibit coronavirus proliferation and growth. *J Virol* 2004; **78**: 5891–9.
- Neuman BW, Stein DA, Kroeker AD et al. Inhibition, escape, and attenuated growth of severe acute respiratory syndrome coronavirus treated with antisense morpholino oligomers. *J Virol* 2005; **79**: 9665–76.

- 13** Munster VJ, Feldmann F, Williamson BN *et al.* Respiratory disease in rhesus macaques inoculated with SARS-CoV-2. *Nature* 2020; **585**: 268–72.
- 14** van den Born E, Stein DA, Iversen PL *et al.* Antiviral activity of morpholino oligomers designed to block various aspects of *Equine arteritis virus* amplification in cell culture. *J Gen Virol* 2005; **86**: 3081–90.
- 15** Zhang YJ, Stein DA, Fan SM *et al.* Suppression of porcine reproductive and respiratory syndrome virus replication by morpholino antisense oligomers. *Vet Microbiol* 2006; **117**: 117–29.
- 16** Sawicki SG, Sawicki DL, Siddell SG. A contemporary view of coronavirus transcription. *J Virol* 2007; **81**: 20–9.
- 17** Pasternak AO, Spaan WJ, Snijder EJ. Nidovirus transcription: how to make sense . . .? *J Gen Virol* 2006; **87**: 1403–21.
- 18** Yang D, Leibowitz JL. The structure and functions of coronavirus genomic 3' and 5' ends. *Virus Res* 2015; **206**: 120–33.
- 19** Khailany RA, Safdar M, Ozaslan M. Genomic characterization of a novel SARS-CoV-2. *Gene Rep* 2020; **19**: 100682.
- 20** Ge Q, Pastey M, Kobasa D *et al.* Inhibition of multiple subtypes of influenza A virus in cell cultures with morpholino oligomers. *Antimicrob Agents Chemother* 2006; **50**: 3724–33.